THE INFLUENCE OF A HYDRIDED LAYER ON THE FRACTURE OF ZIRCALOY-4 CLADDING TUBES

Robert S. Daum
Argonne National Laboratory, Argonne, IL 60439

Douglas W. Bates[1], Donald A. Koss and Arthur T. Motta
The Pennsylvania State University, University Park, PA 16802
([1]Currently with United States Navy)

Abstract

During operation of nuclear power reactors, irradiated Zircaloy™-4 cladding tubes contain circumferentially oriented hydrides concentrated in a layer near the outer surface of the cladding. This study has investigated the effect of such a hydride layer or "rim" located near the outer surface of the cladding tube on the failure of *unirradiated* Zircaloy-4 cladding tubes. Utilizing plane-strain ring-stretch tests with the maximum principal stress along the circumferential or hoop direction, we examined the influence of a hydride rim on the failure of Zircaloy-4 cladding at both room temperature and 300°C. Fracture is found to be sensitive to hydride-rim thickness such that cladding tubes with a hydride-rim thickness >140 μm (≈700 wtppm total hydrogen) exhibit brittle behavior, while cladding tubes with a rim thickness <90 μm (≈600 wtppm) remain ductile. The mechanism of failure is identified as strain-induced sequence of microcrack initiation within the hydride rim, linkage of microcracks to form a long (surface) crack, and subsequent failure of the cladding wall due to either a shear instability or ductile crack growth.

Zircaloy™ is a trademark of Westinghouse Electric Corporation.

Hydrogen Effects on Material Behavior and Corrosion Deformation Interactions
Edited by N.R.Moody, A.W.Thompson, G.S.Was and R.H.Jones
TMS (The Minerals Metals and Materials Society), 2003

Introduction

The mechanical behavior of zirconium-based nuclear fuel cladding degrades during in-reactor service due to a combination of oxidation, hydriding, and radiation damage. To decrease the operating costs of these reactors through the use of longer fuel cycles, and to reduce the volume of waste associated with core reloads, utilities have a strong incentive to extend the use of fuel assemblies to higher burnup levels. Further increases in operating efficiency of power reactors can also be achieved by increasing the coolant outlet temperature. Both of these operating procedures enhance cladding degradation, increasing the likelihood of cladding failure during design-basis accidents.

The reduction of cladding ductility at high levels of fuel burnup is believed to result from a combination of radiation damage, oxidation, and hydriding [*1-3*]. Radiation damage from fast neutrons increases the dislocation density in recrystallized material, causing hardening. However, this increase in dislocation loop density is thought to saturate at relatively low exposures [*3*]. During service, the cladding undergoes oxidation with associated hydrogen pickup. The total amount of hydrogen increases steadily with fuel burnup [*4*], and once the terminal solubility is exceeded, hydride precipitates form in a layer or "rim" near the outer (cooler) surface of the cladding. Thus, during operation the cladding tube form a hydride rim that resides above a substrate that is relatively free of hydrides. Given the texture in the Zircaloy-4 cladding tubes used in light water reactors, the hydride layer consists of aligned, circumferentially oriented hydride platelets [*2,5-7*]. A prediction of the ductility of such cladding tubes must take into account: the density of the hydrides as a layer/rim and the rim thickness, the ability of the hydrides to deform [*6-9*], their circumferential orientation within the layer, and the presence of a relatively unhydrided substrate.

A second condition that affects the sensitivity of high-burnup cladding to hydrogen is the stress state associated with in-service loading. It is well known that elevating the stress triaxiality ratio decreases the fracture strain of recrystallized zirconium alloy sheet containing uniform distributions of hydrides [*8,10*]. In the case of cold-worked and stress-relieved (CWSR) zirconium alloy cladding tubes subject to postulated reactor accidents such as a reactivity-initiated accident (RIA), the interaction between the fuel pellet and the cladding tube forces the cladding to deform under multiaxial tensile stress states; these are generally believed to be in the range $1 \leq (\sigma_\theta/\sigma_z) \leq 2$, where σ_θ is the hoop stress component and σ_z is the axial stress component. In other words, the cladding tube is forced to deform under stress states ranging between equal-biaxial tension ($\sigma_\theta/\sigma_z = 1$) and transverse plane-strain tension ($\sigma_\theta/\sigma_z = 2$ for a plastically isotropic tube). To address this stress-state issue, we have recently developed a "transverse, plane-strain, ring-stretch tension test" [*11,12*]. That test utilizes a double-edge notched ring specimen in which the notches impose a near plane-strain deformation path within the specimen.

While the influence of a *uniform* distribution of hydrides on the tensile ductility of zirconium-based alloys has been studied extensively [*8-10,13,14*], failure behavior when hydrides are non-uniformly distributed in the form of a layer or rim has not been thoroughly addressed, such non-uniform hydride distributions affect cladding failures during RIA testing [*15*] and under burst testing of irradiated Zircaloy-4 cladding tubes [*16*]. Recent experiments based on unirradiated cladding tubes containing hydrides in the form of a rim indicate a significant loss of ductility with (a) increasing hydrogen content [*17*] and/or (b) increasing hydride rim thicknesses [*18*]. These results suggest that a ductile-to-brittle transition occurs with increasing hydride rim thickness. Since the hydride rim initiates a crack early in the deformation process [*15,16,18,19*], fracture mechanics has recently been used to predict failure on the basis of crack propagation [*19,20*]. While this type of analysis can be applied to brittle cladding with

thick hydride rims, failure of cladding with small-thickness hydride rims exhibits significant ductility; importantly, this cladding does not appear to obey fracture mechanics, as the fracture stress approaches the tensile strength of the cladding [*20*]. The physical process controlling the failure of cladding containing thin hydride rims is not understood.

The purpose of this study is to examine the failure behavior of unirradiated Zircaloy-4 cladding tubes that contain hydrides concentrated in the form of a thin layer near the outer surface, typical of high-burnup fuel cladding [*16,21*]. Using "ring-stretch" specimen geometries that impose multiaxial stresses and near plane-strain tension in the hoop direction of the cladding tube, we examine the influence of thin layers of hydrides on the ductility of Zircaloy-4 cladding subject to stress states relevant to potential in-service accidents, such as the RIA.

Experimental Procedures

Material

CWSR Zircaloy-4 cladding tubes were obtained from Sandvik Metals and Westinghouse Electric Corporation with outer diameter of approximately 9.5 mm and wall thickness of approximately 0.56 mm. The grain structure consists of elongated grains with ≈10:1 aspect ratio, oriented parallel to the tube axis and having dimensions of ≈10-15 μm long and ≈1-2 μm thick. As-fabricated Zircaloy-4 possesses a crystallographic texture in which the basal planes tend to align with their basal poles inclined approximately $\pm 40^{o}$ to the normal of the tube surface and oriented towards the tangential direction; the basal and prism pole intensities are up to ten times their random value.

To simulate the hydride distribution in high-burnup cladding, the unirradiated cladding tubes were artificially hydrided in an argon/hydrogen gas mixture at 327°C (600 K) by M. Ozawa at Nuclear Development Corporation. The total hydrogen content was determined by an inert gas fusion technique. The total oxygen content of hydrogen-charged cladding was found to be approximately equal to that of as-fabricated cladding.

Figure 1 shows that the microstructures obtained after such a procedure consist of a relatively high concentration of circumferential hydrides concentrated primarily within a layer near the outer surface of the cladding tube, thus forming a "hydride rim." The thicknesses of the hydride rim varied from specimen to specimen and ranged from approximately 20 to 250 μm. In addition, a few hydrides exist within the "substrate" layer of the cladding tube below the hydride rim. It is significant that the hydride microstructure shown in Fig. 1 is similar to that observed in high-burnup fuel cladding [*15,17*]. To isolate the effect of the substrate on hoop tensile ductility, a few specimens that originally had hydride rims were machined to remove the layer.

Mechanical Testing

To impose a biaxial stress state such that hoop extension of the cladding occurs by through-thickness slip, we used the double edge notched "transverse plane-strain ring-stretch" specimen shown in Fig. 2 and described in detail elsewhere [*11,12*]. The specimen uses the constraints of the two notches to force the central region of the gauge section to deform such that little contraction occurs across the specimen width (i.e., along the tube axis). As a result, near plane-strain deformation condition is achieved, as has been supported by finite element modeling and by measurements of the local ratio of thickness to hoop strain [*11*].

Microhardness indentations were used to determine strains on a local basis along the specimen gauge length. This method has an accuracy of ±0.01 (±1%) for strain measurements.

Two measures of cladding failure were used: (a) the "limit strain" (ε_{limit}) is defined as the "uniform" deformation in the gauge section at material failure and is calculated by numerical integration from the as-measured strain distribution and (b) the "fracture strain" (ε_{frac}) defined as the local strain as determined over a 0.2-mm element containing the fracture surface. The tests

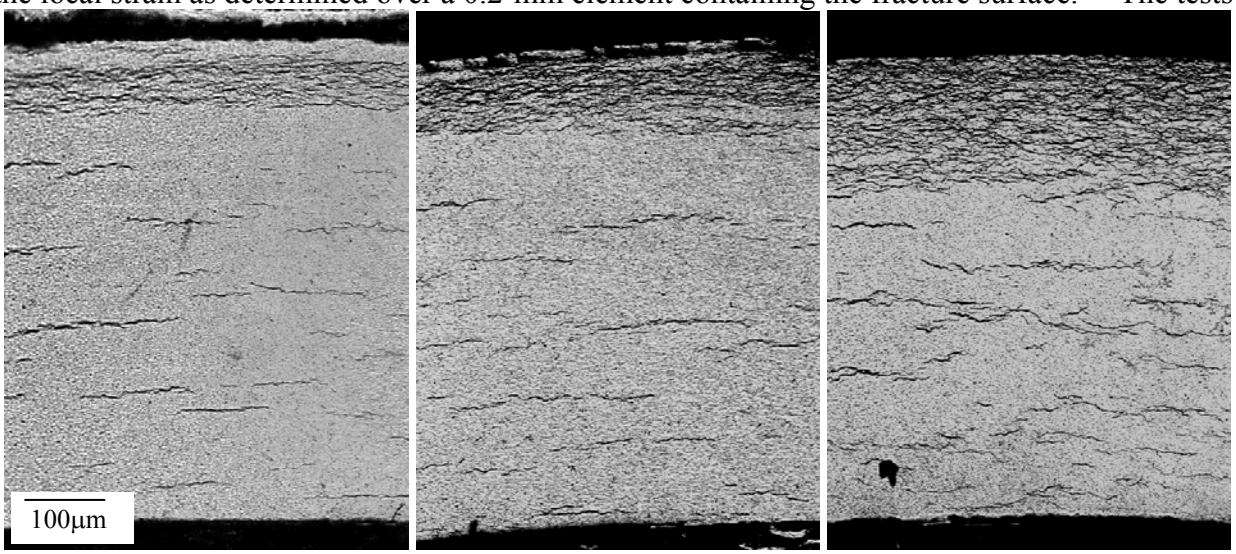

(a) (b) (c)

Figure 1: Light micrographs showing hydride microstructure and distribution within Zircaloy-4 cladding tubes with hydride layer thicknesses of (a) 80, (b) 100, and (c) 180 μm.

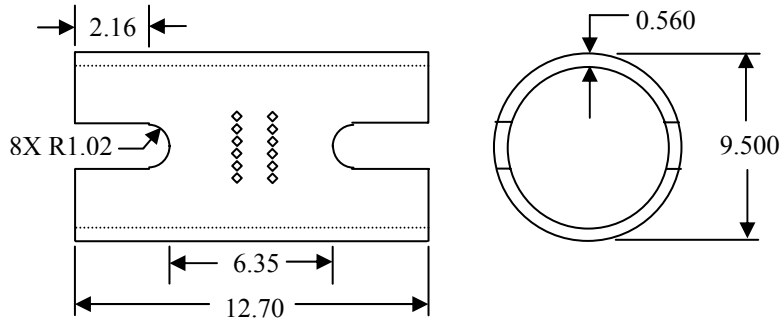

Figure 2: Plane-strain ring-stretch test specimen with microhardness indentation arrays for determining local strains (all dimensions are in mm and not-to-scale).

were performed at an initial strain rate of $\approx 10^{-3}$/s, using loading fixtures consisting of two "D-shaped" die inserts that transmit the displacement to the specimen. To promote uniform deformation along the gauge section and limit frictional effects, a combination of Teflon™ tape and vacuum grease was used to lubricate the interface between the die inserts and the inner surface of the cladding specimen. Tests on unirradiated/unhydrided specimens using the above procedure confirm relatively uniform deformation along a gauge section somewhat greater than 2 mm long along the circumferential direction shown in Fig. 2.

Results and Discussion

On the Failure Process

For cladding that has a dense layer of hydrides in the form of a rim near its outer surface, as shown in Fig. 1, our observations suggest the following failure process. With the exception of one observation at 300ºC, cracks initiate within the hydride rim upon yielding of the cladding tube, as indicated in Fig. 3 (note that micro-cracks seldom initiate at microhardness indents). Results from several specimens show that the crack density increases with decreasing hydride

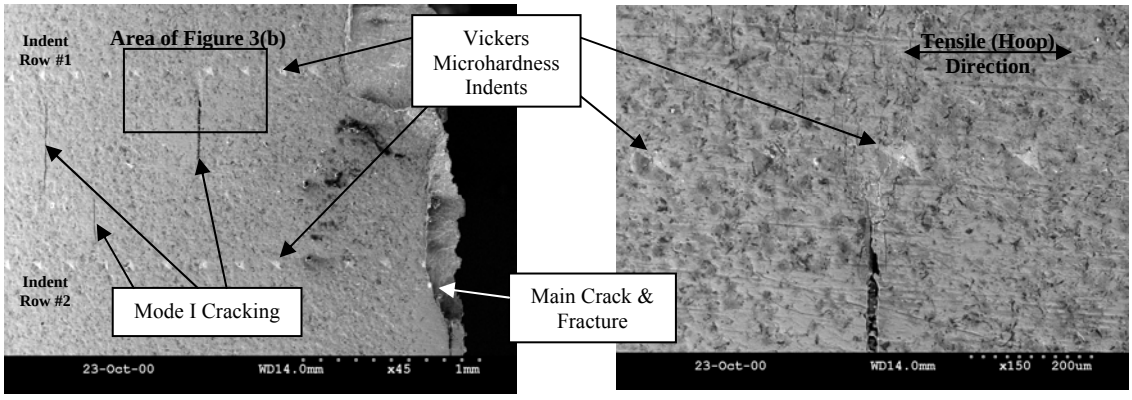

(a) (b)

Figure 3: Scanning electron micrographs at (a) low magnification and (b) higher magnification showing surface cracks initiating within a 148μm thick hydride rim after testing at room temperature.

rim thickness such that only a few deep micro-cracks form within the cladding with thick hydride layers (≥ 140 μm), while a high density of short (length ≤ 0.5mm) microcracks form within the thin hydride layers. This crack density effect appears to be related to the influence of the free surface created by the crack flanks in inhibiting the initiation of neighboring cracks.

The fracture path also differs in the thick- and thin-hydride rim cladding. In *thin* hydride samples that fail by plastic collapse, the linking of multiple microcracks creates a long surface crack (> 2-3 mm) that, while not deep, is relatively planar. In this instance, strain accumulates while the short microcracks, which are blunted in the relatively ductile substrate, link into a long macrocrack that eventually propagates through the cladding thickness. As shown in Fig. 4, eventual fracture of the uncracked ligament occurs as a result of either damage-induced fracture (at room temperature; see Fig. 4a) or shear localization (at 300°C; see Fig. 4b). At room temperature, damage-induced fracture occurs because the strain to nucleate, grow, and coalesce voids (i.e., damage accumulation) is less than that required to develop a localized neck. The damage-accumulation fracture will also be favored by an increased density of hydrides within the uncracked ligaments, such as might occur if the hydride layer is thick. In contrast, localized necking and shear failure of the uncracked ligament will likely be favored at 300°C (Fig. 4b), where an increase in damage-induced fracture strain enables localization to develop [*11*].

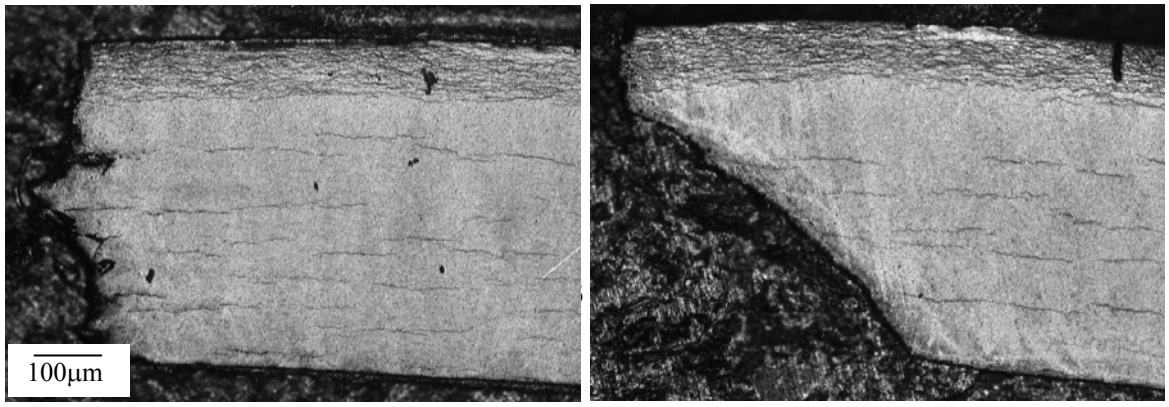

(a) (b)

Figure 4: Transverse fracture profiles of cladding with a hydride rim tested at (a) room temperature and (b) 300°C.

Based on the above interpretation, we suggest that fracture of cladding with a hydride rim occurs by a multistage process: (1) initiation of short microcracks within the hydride rim, (2) growth and linkage of microcracks into a long surface crack (along the tube axis), and (3) cladding fracture due to the propagation of the long surface crack by either a damage accumulation process (at room temperature) or failure of the relatively hydride-free ligament by shear instability (at 300°C). This failure sequence is discussed below:

1. Initiation of microcracks. Our observations indicate that microcracks (≤ 0.5 mm surface length) initiate at very small strains (essentially zero strain, as in previous research [*18*]). Also, the density of these microcracks decreases with increasing hydride layer thickness, as described above. Thus, thick hydride layers (> 150 μm) initiate a single deep crack which extends across the entire specimen (≈ 6 mm), resulting in near-brittle behavior, as can be predicted by fracture mechanics analysis [*19,20*].
2. Micro-crack linkage. When the hydride rim is thin (< 90 μm thick), the growth and linkage of microcracks into a long (surface) crack results in cladding ductility. This second stage appears to depend on both the density of cracks *and* their depth. A high density of very shallow (≈ 20 μm thick) microcracks will link rather quickly with strain, forming a long (> 2 to 3 mm) but shallow surface crack. In contrast, a lower density of more widely spaced and *non-coplanar* surface cracks of *intermediate* depth (i.e., ≈ 75 μm) will link with difficulty. In this case, cladding ductility also occurs during this strain-induced linking of moderately deep cracks into a tortuous, long surface crack.
3. Failure of the substrate. Failure of the cladding substrate below the hydride rim depends in a sensitive manner on rim depth, with strain to failure increasing as hydride-rim depth decreases. The through-thickness growth of shallow cracks in cladding with a thin hydride layer is difficult, and significant crack opening displacement (and material ductility) occurs before substrate fracture occurs due to damage accumulation at room temperature or shear instability at 300°C at stresses significantly greater than the yield stress. Cladding with a hydride-rim of medium depth (≈ 75 μm) has a tendency to link microcracks that are *not co-planar* and to form a tortuous fracture path through the substrate; ductility results as the failure stress exceeds the yield stress. Finally, cladding with thick hydride layers initiates a long (> 3 mm) surface crack that propagates easily as a "deep", planar crack through the substrate, near-brittle behavior of the cladding results, likely obeying a criterion based on hydride rim thickness/crack "depth" [*19,20*].

Effect of Hydride Layers on Ductility

Failure of the hydrided Zircaloy cladding was determined on the basis of strain distributions of failed specimens, as shown in Fig. 5a (where $\varepsilon_{\theta\theta}$ is the true major strain and y_f is the total gauge length in the hoop direction). It should be noted that our strain values are based on elements initially 0.2 mm long. Thus, Fig. 5b indicates finite strain levels adjacent to a crack over the 0.2 mm length, even though we expect near zero strains immediately adjacent to the crack.

After cracks initiate within the hydrided rim, cladding hoop extension occurs before deformation localization/fracture develops within the uncracked ligament. Therefore, the value of ε_{limit}, the far-field strain at the failure, includes the sum of the displacements accumulating during macrocrack formation and subsequent deformation in the uncracked ligaments but not

those crack opening displacements associated with arrested microcracks and the macrocrack. Figure 5b indicates $\varepsilon_{limit} \cong 0.06$ as the level of strain present along the cladding tube at locations between cracks. The ε_{limit} value may be viewed as a lower limit of the cladding failure strain for unirradiated, hydrided cladding.

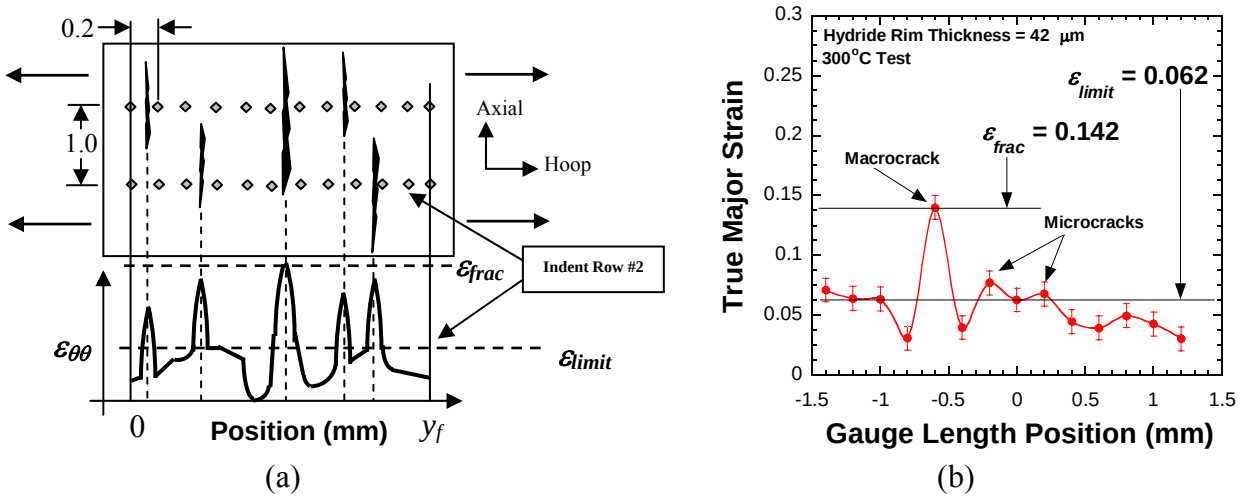

Figure 5 – (a) Schematic of the influence of microcracks on the strain distribution along Indent Row #2 (dimensions in millimeters and not-to-scale) and (b) the measured strain distribution at cladding fracture for a plane-strain ring-stretch specimen with hydride layer thickness of 42 μm tested at 300°C.

The cladding fracture strain, ε_{frac}, is the measure of the local strain required for cladding fracture. We present in Fig. 6 the dependence of both the limit strain (Fig. 6a) and the fracture strain (Fig. 6b) on thickness of the hydride layers in Zircaloy-4 cladding tubes deformed in near plane-strain tension to failure at room temperature and 300°C. The most important trend in Fig. 6 is the obvious dependence of cladding ductility on hydride-layer thickness. At both room temperature and 300°C, the ε_{limit} values (Fig. 6a) indicate a gradual ductile-to-brittle transition with increasing hydride layer thickness. Specifically, cladding with hydride rims of thicknesses ≥140 μm show little or no plastic deformation to failure. In view of the fact that the experimental accuracy of our measurements of local strain is ±0.01 (±1%), these cladding tubes are essentially brittle. At the 100 μm hydride thickness level, there may be a small level of plastic deformation to the cladding prior to failure. However, cladding samples with hydride-rim thicknesses <90 μm are distinctly ductile, with hoop limit strains of roughly 0.04 or greater.

The ductile-to-brittle transition is further defined by considering values of ε_{frac}, as shown in Fig. 6b. Consistent with limit strain behavior, specimens with hydride rim thicknesses ≤85 μm show fracture strains greater than 0.1 (10%), while thicknesses >100 μm show $\varepsilon_{frac} < 0.05$. It is not straightforward to relate these failure strain values to cladding fracture under an RIA transient. If localization of strain is induced by friction resulting from pellet-cladding interactions, ε_{frac} could be an important parameter in characterizing cladding failure susceptibility. On the other hand, if fuel pellet-cladding friction is minimal, ε_{limit} could be the more appropriate failure criterion.

It is tempting to consider results such as those in Fig. 6 on the basis of hydrogen content, as has been done in many previous studies [*8,10,13,14*]. Typically, these studies have associated a significant loss of ductility with increasing hydrogen content, such that the factor controlling

the ductile-to-brittle transition is assumed to be the overall hydrogen level. In the present study, the brittle Zircaloy-4 cladding with *thick* hydride rims had total hydrogen contents ≥500 wtppm. However, significant ductility was also observed in specimens with *thin* hydride layers, where the cladding had a total hydrogen content ≥700 wtppm. Furthermore, our present data indicate that cladding specimens with hydrogen content in the 500-800 wtppm range but different hydride layer thicknesses fail at widely varying values of ductility. Thus, for the case of a hydride rim, we conclude that the total hydrogen content is not the best measure of cladding ductility, but that the ductile-to-brittle transition is better defined by hydride rim thickness. Such a result contrasts with the case for uniformly distributed hydrides across the entire cladding thickness, in which the factor controlling the ductile-to-brittle transition is the overall hydrogen level.

Finally, to confirm that the ductility losses presented above in Fig. 6 are indeed caused by the presence of the hydride rim, we present Fig. 7. This figure is based on the behavior of *sibling* specimens with the hydride rim intact and mechanically removed. These results indicate that the previously brittle cladding is ductile once the hydride layer is removed. Removing the hydride rim restores the ε_{limit} and ε_{frac} values to levels close to those determined for unhydrided cladding.

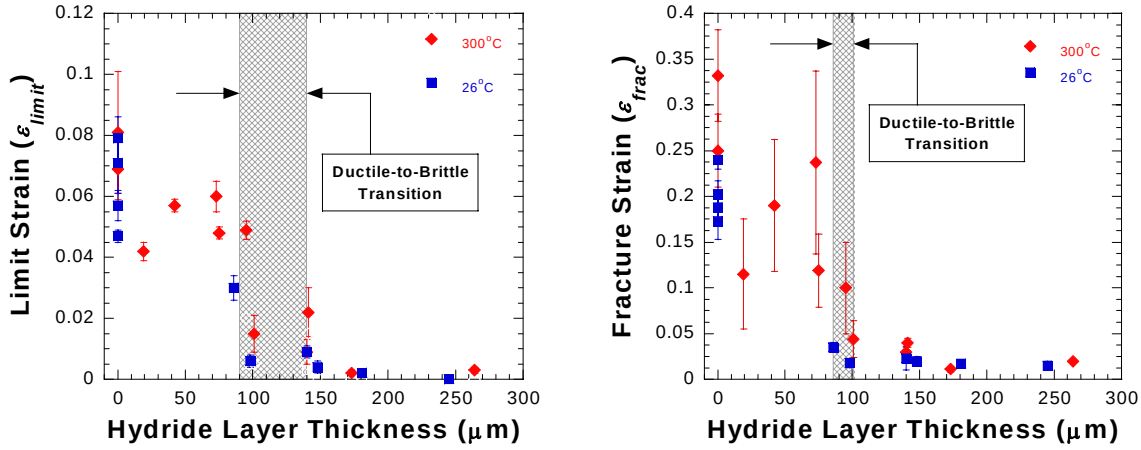

(a) (b)

Figure 6: (a) Limit strain (ε_{limit}) and (b) fracture strain (ε_{frac}) as a function of temperature and hydride layer thickness.

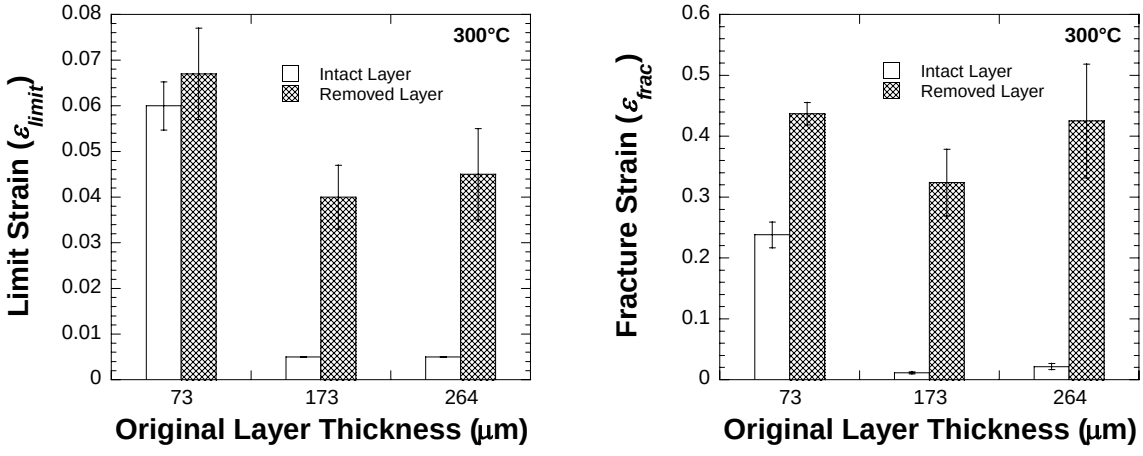

(a) (b)

Figure 7: (a) Limit strain (ε_{limit}) and (b) fracture strain (ε_{frac}) at 300ºC as a function of original hydride layer thickness for cladding with intact and removed layer.

Summary

We have examined the fracture behavior of Zircaloy-4 cladding tubes containing hydrides precipitated in the form of a hydride rim near the outer surface. Utilizing a ring-stretch test that imposes a multiaxial stress state such that near plane-strain tension is achieved in the cladding hoop direction, we conclude the following:

1. Cladding ductility is very sensitive to hydride-rim thickness at both room temperature and 300°C. This sensitivity is manifested in a loss of ductility with increasing hydride rim thicknesses, such that the cladding is ductile when the hydride rim thickness is less than 90 μm, but it is brittle at hydride rim thicknesses of approximately 140 μm and greater. Our results also indicate that cladding containing <500 wtppm total hydrogen remains ductile regardless of whether hydrides are present in the form of a hydride rim or uniformly distributed hydrides. Moreover, the hydride rim thickness appears to be a more suitable parameter than hydrogen content for determining a ductile-to-brittle transition in cladding with a hydride rim.
2. The failure mechanism of hydrided cladding involves three stages: (1) microcrack initiation with crack depth equal to hydride rim thickness, (2) growth and linkage of microcracks into a long surface crack, and (3) failure of the relatively hydride-free ligament by either crack growth due to damage accumulation (room temperature) or the formation of a shear instability beneath a blunted crack (300°C). Since microcracks initiate at roughly zero strain, the cladding ductility at small hydride rim thicknesses appears to be a result of the plastic strain necessary to link microcracks into a long surface crack, as well as the strain needed to propagate the cracks through the cladding thickness by either damage accumulation or shear instability.

Acknowledgments

We thank Mr. Ozawa, of NDC in Japan, for his preparation of tubing samples with controlled hydride rims. We thank Ross Bradley at Sandvik Metals for supplying the Zircaloy cladding tubes used in this study. R.S. Daum would also like to thank Terri Bray, Michael Billone, David McGann, and Jakub Dobrzynski of the Irradiation Performance Section at Argonne National Laboratory for technical discussions and experimental assistance. This research was supported by the U.S. Nuclear Regulatory Commission, Office of Nuclear Regulatory Research.

References

1. R.O. Meyer et al., "A Regulatory Assessment of Test Data for Reactivity Initiated Accidents," Nuclear Safety, 37 (1996), 872-387.

2. H.M. Chung, F.L. Yaggee, and T.F. Kassner, "Fracture Behavior and Microstructural Characteristics of Irradiated Cladding," 7th Inter. Sym. on Zr in the Nuclear Industry (West Conshohocken, PA: ASTM, 1987), 775-801.

3. C. Lemaignan and A.T. Motta, "Zr in Nuclear Applications," Nuclear Materials, 10 (B) (1994), 1-51.

4. J.P. Mardon et al., "Update on the Development of Advanced Zr Alloys for PWR Fuel Rod Claddings," ANS Proc. of Inter. Topical Mtg. on LWR Fuel Performance (La Grange Park, IL: ANS, 1997), 405-412.

5. C.E. Ells, "Hydride Precipitates in Zr Alloys," J. of Nuclear Materials, 28 (1968), 129-151.

6. C.E. Coleman and D. Hardie, "The Hydrogen Embrittlement of Alpha Zr--A Review," J. of Less-Common Metals, 2 (1966), 168-185.

7. H.M. Chung et al., "Characteristics of Hydride Precipitation and Reorientation in Spent-Fuel Cladding," 13th Inter. Sym. on Zr in the Nuclear Industry (West Conshohocken, PA: ASTM, 2002), in print.

8. M. Grange, J. Besson, and E. Andrieu, "Anisotropic Behavior and Rupture of Hydrided Zr-4 Sheets," Metallurgical and Material Transactions A, 31A (2000), 679-690.

9. M. Kuroda et al., "Influence of Precipitated Hydride on the Fracture Behavior of Zr Fuel Cladding Tube," J. of Nuclear Science and Technology, 37 (8) (2000), 670-675.

10. Y. Fan and D.A. Koss, "The Influence of Multiaxial States of Stress on the Hydrogen Embrittlement of Zr Alloy Sheet," Metallurgical Transactions A, 16A (1985), 675-681.

11. T.M. Link, D.A. Koss, and A.T. Motta, "Failure of Zr Cladding under Transverse Plane-Strain Deformation," Nuclear Engineering and Design, 186 (1998), 379-394.

12. R.S. Daum et al., "Mechanical Property Testing of Irradiated Zr Cladding under Reactor Transient Conditions," 4th Inter. Sym. on Small Specimen Test Tech. (West Conshohocken, PA: ASTM, 2002), in print.

13. J.B. Bai, C. Prioul, and D. Francois, "Hydride Embrittlement in Zr-4 Plate: Part I," Metallurgical and Materials Transactions A, 25A (1994), 1185-1197.

14. P. Bouffioux and N. Rupa, "Impact of Hydrogen on Plasticity and Creep of Unirradiated Zr-4 Cladding Tubes," 12th Inter. Sym. on Zr in the Nuclear Industry (West Conshohocken, PA: ASTM, 2000), 399-422.

15. T. Fuketa et al., "Fuel Failure and Fission Gas Release in High Burnup PWR Fuels Under RIA Conditions," J. Nuclear Materials, 248 (1997), 249-256.

16. A.M. Garde, G.P. Smith, and R.C. Pirek, "Effects of Hydride Precipitate Localization and Neutron Fluence on the Ductility of Irradiated Zr-4," 11th Inter. Sym. on Zr in the Nuclear Industry (West Conshohocken, PA: ASTM, 1996), 407-430.

17. T. Fuketa et al., "Behavior of PWR and BWR Fuels During Reactivity Initiated Accidents", ANS Proc. of Inter. Topical Mtg. on LWR Fuel Performance (La Grange Park, IL: ANS, 2000), 1135-1147.

18. R.S. Daum et al., "On the Embrittlement of Zircaloy-4 under RIA-Relevant Conditions," 13th Inter. Sym. on Zr in the Nucl. Industry (West Conshohocken, PA: ASTM, 2002), in print.

19. M. Kuroda et al., "Analysis of the Fracture Behavior of Hydrided Fuel Cladding by Fracture Mechanics", Nuclear Engineering and Design, 203 (2001), 185-194.

20. S. Yamanaka et al., "Analysis of the Fracture Behavior of Hydrided Cladding Tube at Elevated Temperatures by Fracture Mechanics", J. Alloys and Compounds, 330-332 (2002), 400-403.

21. T. Fuketa et al., "NSRR/RIA Experiments with High Burnup PWR Fuels," ANS Proc. of Inter. Topical Mtg. on LWR Fuel Performance (La Grange Park, IL: ANS, 1997), 669-676.